ACS OMEGA

http://pubs.acs.org/journal/acsodf

Article

Photo-Luminescent Photonic Crystals for Anti-Counterfeiting

Chenjing Xu, Changgeng Huang, Dongpeng Yang,* Li Luo,* and Shaoming Huang*

Cite This: *ACS Omega* 2022, 7, 7320−7326

Read Online

ACCESS | Metrics & More | Article Recommendations | Supporting Information

ABSTRACT: The conventional photonic crystals (PCs) are usually prepared by the self-assembly of silica or polystyrene particles. However, their applications are limited significantly due to the lack of the functions of the building blocks. Here, a new kind of photo-luminescent photonic crystals (PLPCs) with brilliant PL and structural colors were prepared by the self-assembly of dye-doped silica particles. The PL and structural colors of PCs can be well-controlled by altering the species of dyes and the size of the particles, respectively. Based on these advantages, PLPC patterns with encrypted information were fabricated through the combination of PLPCs and PCs with similar structural colors but diverse PL colors. These patterns can reversibly hide and display the encrypted information under sunlight and UV illumination, respectively. This work paves a new way for constructing functional PCs and will promote their applications in anti-counterfeiting, smart labels, and optical devices.

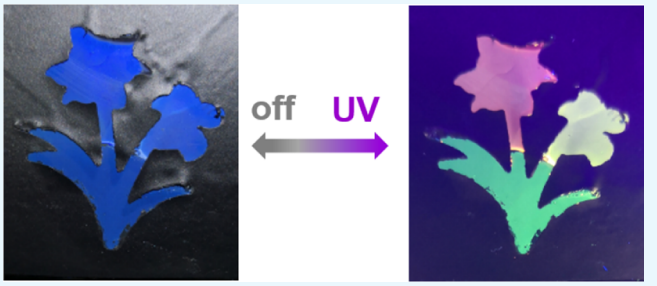

1. INTRODUCTION

Photonic crystals (PCs)[1−3] with brilliant structural colors have attracted wide attention due to their growing applications in the fields of displays,[4−10] printings,[11−17] pigments,[18−25] sensors,[26−32] coding−decoding,[33−36] photocatalysis,[37,38] and anti-counterfeiting.[39−47] As a member of PCs, colloidal PCs self-assembled from the colloidal particles have attracted considerable interest since the particles can be fabricated in a large scale with low cost in an efficient way. In order to prepare PCs with high qualities, colloidal particles should fulfill the following requirements: (1) the size of particles with the coefficient of variation should be less than 5%; (2) the size of the particles could be well-controlled (100−300 nm) to tune the reflection wavelengths and structural colors of PCs; and (3) the intrinsic colors of particles should not have influences on the structural colors of PCs. Actually, it is widely accepted and experimentally proved that the silica or polystyrene particles with monodispersed morphology, tunable sizes, and white colors are the mostly suitable building blocks for the fabrication of PCs. However, these particles lack functions, greatly limiting the practical applications of PCs. The combinations of new functions especially other optical materials (inorganic materials or dyes) into PCs would offer new opportunities for extending the applications of PCs in anti-counterfeiting and information protection.

One possible way to fabricate functional PCs is to mix the optical materials with the building blocks and then assemble them together. However, the direct introduction of optical materials into the colloidal solution would probably (1) disturb the assembly behavior of the colloidal particles and thus the order degrees of PCs and (2) cause the random distributions of the optical materials into PCs. Therefore, the direct encapsulation of optical materials into the internal regions of the colloids would be an applicable way. However, it is still a big challenge to prepare functional colloids with uniform and tunable sizes. Recently, our group have successfully prepared $YOHCO_3/Eu$[48] and Y_2O_3/Eu[49] colloids, which can self-assemble into photo-luminescent photonic crystals (PLPCs) and can be used for anti-counterfeiting. However, only amorphous structures can be obtained due to the large size distributions of the particles, resulting in unfavorable faintly structural colors. The fabrications of PC with highly ordered structures, brilliant structural colors, and tunable photo-luminescent (PL) colors are extremely important and urgently desired.

In this work, a new kind of PLPCs with opal structures, bright structural colors, and PL colors were fabricated by the self-assembly of dye-doped SiO_2 particles. The organic dyes are covalently bonded into the network of SiO_2 particles through the simple fabrication. Except for the PL colors, the dye-doped SiO_2 particles show similar properties compared to that of conventional Stöber SiO_2 particles, which is crucial to the highly ordered structures of PLPCs. The reflection wavelength and corresponding structural colors of PLPCs can be well controlled by altering the size of the dye-doped SiO_2 particles,

Received: December 19, 2021
Accepted: February 2, 2022
Published: February 19, 2022

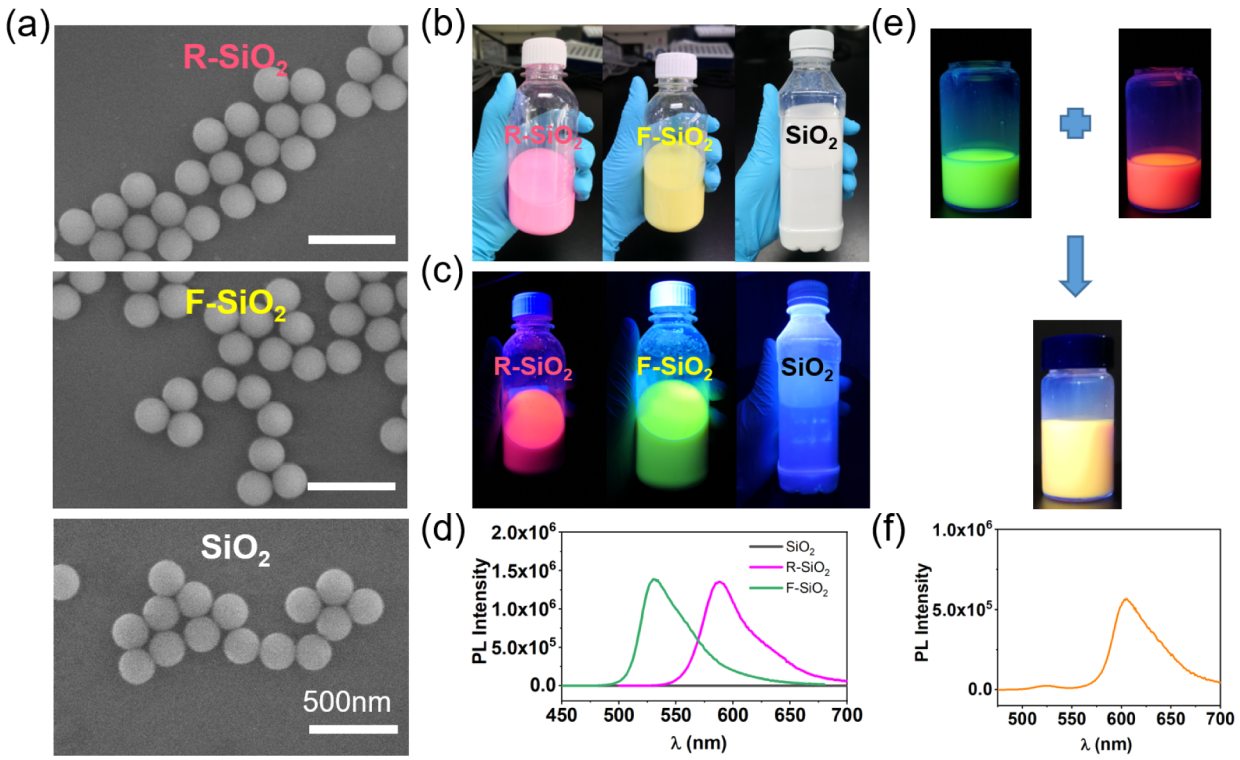

Figure 1. (a) SEM images of R−SiO_2, F−SiO_2, and SiO_2 particles. Digital photographs of colloidal solution under (b) ambient light and (c) UV illumination. (d) PL spectra of colloidal solutions. (e) Digital photographs and (f) corresponding PL spectrum of colloidal solution with new yellow PL color through the mixing strategy. The concentration of colloidal solution in (b,e) is 200 mg/mL.

while their PL colors can be tailored by adjusting the species of dyes. Moreover, a new PL color can be achieved by mixing SiO_2 particles with different dyes. Based on these advantages, photonic patterns with encrypted information were fabricated, which could reversibly hide and show the information at normal condition and UV light, respectively. This work provides a new view for fabrication of PLPCs and will promote the applications of PCs in the field of displays, optical coatings, and anti-counterfeiting.

2. RESULTS AND DISCUSSION

The PLPCs were fabricated by the self-assembly of dye-doped silica particles into opal structures. Apparently, the preparation of the PLPCs should fulfill the following requirements: (1) the dye-doped silica particles should possess uniform size in order to self-assemble into PLPCs; (2) the PL and structural colors of the PLPCs can be controlled independently by different parameters; and (3) the photonic band gap of the PLPC has a negligible effect on its PL properties. The key to satisfy all these requirements is to synthesize silica particles with high uniformity, tunable size, and PL colors.

2.1. Dye-Doped SiO_2 Particles. Prior to the fabrication of PLPCs, the dye-doped silica particles were first prepared by the co-hydrolysis of tetraethyl orthosilicate (TEOS) and dye-modified (3-aminopropyl)triethoxysilane (APS) in the presence of ethanol, water, and ammonium hydroxide. Here, fluorescein isothiocyanate isomer I (FTIC) and rhodamine B isothiocyanate (RITC) are used as the typical dyes to synthesize of dye-doped silica particles since these dyes possess isothiocyanate groups that can form covalent bonds with the amidogen groups of APS through the click reactions. Moreover, these dyes are commercially available, which will facilitate large-scale fabrications. For easy discussion, the RITC- and FITC-doped silica particles are denoted as R−SiO_2 and F−SiO_2, respectively. As presented in Figure 1a, both R−SiO_2 and F−SiO_2 particles have uniform shapes and sizes. The mass fractions of RTIC and FITC of R−SiO_2 and F−SiO_2 particles are about 0.05 and 0.19%, respectively. For comparison, the Stöber SiO_2 particles were also synthesized with similar synthetic protocols except that the TEOS was used as the only source material of silica particles. The size of R−SiO_2, F−SiO_2, and SiO_2 particles is 210, 208, and 208 nm, respectively, indicating that the incorporation of dyes into silica particles has a negligible effect on the uniformity and size of silica particles. Different from the white color of SiO_2 particles (Figure 1b,c), the R−SiO_2 and F−SiO_2 colloidal solutions exhibit colorful appearances under ambient light due to the existence of dyes. When exposed to the UV light, the R−SiO_2 and F−SiO_2 exhibit bright red and yellow PL colors with peak positions located at 522 and 590 nm (Figure 1d), respectively. In striking contrast, no obvious PL color of the SiO_2 colloidal solution can be observed.

The RITC molecules are chemically doped into the network of silica particles with strong covalent bonding, which means that the RITC molecules will not escape from the particles and thus possess a stable fluorescent intensity. The R−SiO_2 particles were separated from the solution by centrifuging after being stored for 1 year. The transparent supernatant solution (Figure S1) firmly demonstrates the stability of the network of the R−SiO_2. The mass fraction of RITC in R−SiO_2 particles is as low as about 0.05%, implying that the RhB molecules are probably isolated from each other and thus avoid the aggregation of the dye molecules efficiently. For example, the fluorescence of the R−SiO_2 particles is much brighter than that of RITC powder (Figure S2), strongly supporting the above assumption. The mass ratio of the dye molecules will

https://doi.org/10.1021/acsomega.1c07150
ACS Omega 2022, 7, 7320−7326

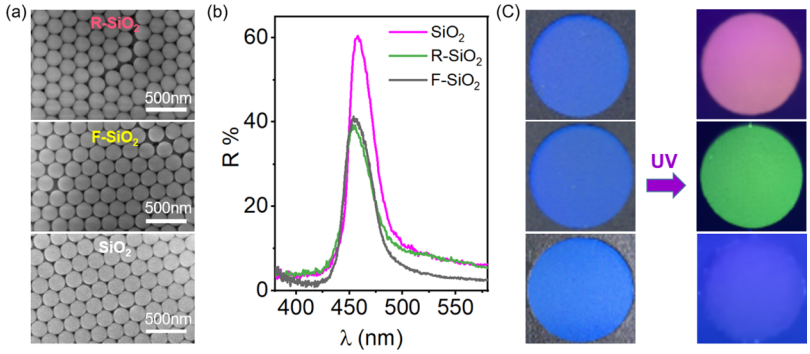

Figure 2. (a) SEM images, (b) reflection spectra, and (c) digital photographs of PLPCs assembled from R−SiO_2, F−SiO_2, and SiO_2 particles. The diameter of the samples in (c) is 1 cm.

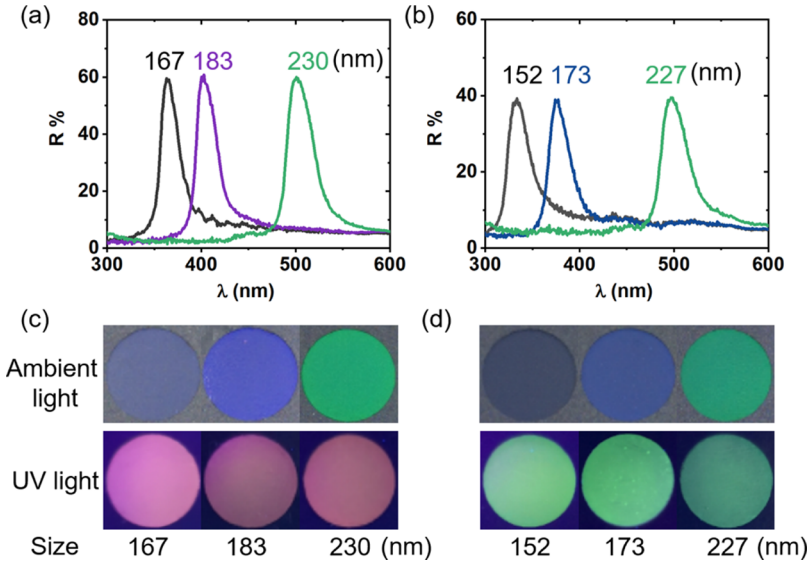

Figure 3. (a,b) Reflection spectra and (c,d) digital photographs of PLPCs assembled from (a,c) R−SiO_2 and (b,d) F−SiO_2 particles with different sizes. The diameter of the samples in (c,d) is 1 cm.

affect the PL intensity. As shown in Figure S3, we have prepared three R−SiO_2 particles with the mass ratio of dyes of 0.05, 0.1, and 0.5. Apparently, the PL intensity of the colloidal solution depends on the mass ratio of dyes. The PL brightness increases along with the increase in the mass ratio of dyes, while the PL hues of the three samples are similar. These results suggest that the mass ratio of the dye molecules majorly determines the brightness of the PL intensity of the colloidal solutions rather than their PL colors.

2.2. Adjusting the Size and PL Color of Dye-Doped SiO_2 Particles. Similar to the Stöber SiO_2 particles, the size of the dye-doped SiO_2 particles can be tailored by changing the amount of TEOS. For example, R−SiO_2 particles in the size of 167, 183, and 230 nm (Figure S4) can be prepared when 6, 5.4, and 4.3 mL of TEOS are used, respectively. These particles possess uniform sizes and similar PL colors under illumination of UV light.

As discussed above, the PL color of the SiO_2 particles can be well controlled by changing the species of dyes. However, these two kinds of dye-doped silica particles only result in red and green colors under UV irradiation, which may limit their applications. To deal with this problem, one can obtain new PL colors by mixing the silica particles embedded with different dyes. As illustrated in Figure 1e,f, the colloidal solution showing brilliant yellow PL color under UV light can be achieved when the R−SiO_2 and F−SiO_2 particles are mixed with the mass ratio of 1:1. The corresponding PL spectrum proves that the yellow color of the solution with mixed particles originates from the overlap of red and green PL colors. In fact, we have found that the PL positions of the (f) is quite different from the colloidal solution of pure R- or F−SiO_2. It is beyond our abilities to explain this. The mechanism of this phenomenon needs further investigations and efforts. Different mixed colors can be further obtained when using different proportions (Figure S5). Here, three mixed colloidal solutions with the mass ratios of F−SiO_2/R−SiO_2 of 80:20, 50:50, and 25:75 are first prepared, which show yellow, orange, and pink colors under ambient light illumination, respectively. After exposing to UV light, PL colors of yellow green, orange, and red colors can be obtained, and corresponding PL spectra also support these results. Obviously, the PL color of mixed solution turns from green to red with the increase in the mass ratio of R−SiO_2 from 0 to 100%. These results demonstrate that the dye-doped silica particles with highly tunable sizes and PL properties can be easily fabricated.

2.3. PLPCs and Their Optical Properties. PLPCs were fabricated by the self-assembly of dye-doped silica particles. Here, R−SiO_2, F−SiO_2, and SiO_2 particles with similar sizes (~210 nm) are used as the building blocks for the preparation of PLPCs. Briefly, the particles are first dispersed in ethanol,

https://doi.org/10.1021/acsomega.1c07150
ACS Omega 2022, 7, 7320−7326

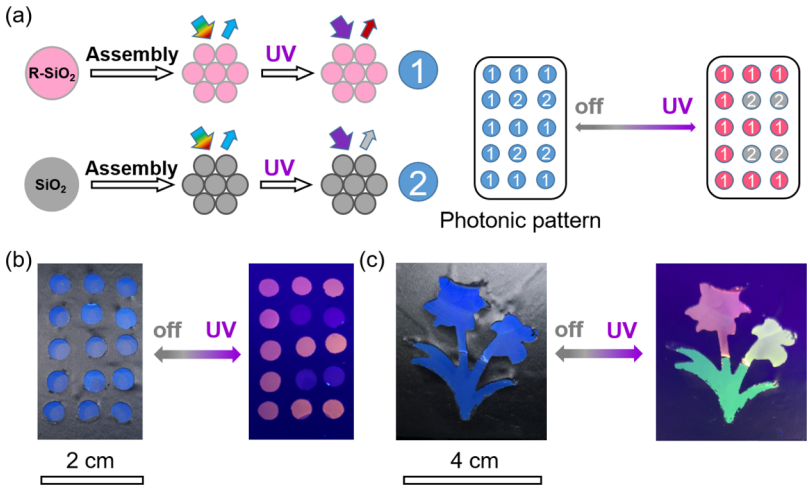

Figure 4. (a) Schematic illustration of fabrication of photonic patterns based on the combinations of PLPCs and PCs. (b,c) Digital photographs of photonic patterns under ambient light and UV light.

followed by drying at 333 K. The particles would self-assemble into ordered structures during the evaporation process. Figure 2a shows the scanning electronic microscopy (SEM) images of the PLPCs assembled from the R−SiO_2 and F−SiO_2 particles and PCs assembled from SiO_2 particles. Apparently, for the PLPCs and PCs, the particles are closely packed to each other into long-range ordered and face-centered cubic (FCC) structures with the (111) planes exposed. Correspondingly, the reflection wavelengths (Figure 2b) of PLPCs and PCs are located at around 461 nm because these particles have similar particle sizes. The reflection peak position of PLPCs can be calculated by Bragg's law (eqs 1 and 2).

$$m\lambda = 1.633D\sqrt{n^2 - \sin^2\theta} \quad (1)$$

$$n^2 = n_s^2 f_s + n_a^2 f_a \quad (2)$$

where m and λ are the diffraction order and reflection wavelength, respectively. D is the center-to-center spacing between neighboring particles, which is equal to the diameter of silica particles, respectively. θ is the angle between the reflected beam and the normal. The n, n_s, and n_a are the refractive index of PCs, SiO_2 particles, and air, respectively. The f_s and f_a are the volume fraction of SiO_2 particles and air, respectively. Here, the λ of the PLPC is calculated to be 460 nm, in good agreement with the result of its reflection spectra. Moreover, the intense reflectance of these PLPCs further proves their highly ordered structures. The long-range ordered structures of PLPCs can be attributed to the strong repulsions between the silica particles.

The PLPCs appear blue similar to that of PCs (Figure 2c), owing to their reflection peak positions located at blue color regions. After being exposed to UV light, these PLPCs show brilliant red and green colors similar to that of their colloidal solution, while no PL color can be observed from the PC sample.

2.4. Adjusting the Structural Color of PLPCs. Like the traditional PCs, the reflection wavelength and structural color of PLPCs can be controlled by altering the size of the dye-doped silica particles. For instance (Figure 3a,c), PLPCs with reflection wavelengths located at 365, 400, and 502 nm and corresponding transparent, violet, and green colors can be obtained when R−SiO_2 particles in the size of 167, 183, and 230 nm are used, respectively. Under UV illumination, these PLPCs show bright red colors, indicating that the structural color can be independently tuned regardless of their PL properties. Similarly, PLPCs (Figure 3b,d) with reflection wavelengths located at 333, 376, and 497 nm and corresponding transparent, violet, and green colors can be obtained when F−SiO_2 particle in the size of 152, 172, and 227 nm are used, respectively. It should be noted that the color brightness of the PLPC with the reflection wavelength located at around 502 nm is much lower than that of other PLPCs, probably due to the prevention of PL emission of FITC by the photonic band gap near the emission of FITC. This result suggests that the photonic band gap of PLPCs may have significant influence on its PL intensity. In this regard, it is better to fabricate PLPCs with large contrast between their reflection and PL peak positions.

The above results demonstrate that PLPCs with tunable reflection wavelengths, structural colors, and PL colors can be easily prepared. In particular, the dual optical properties of PLPCs can be independently controlled through rational design of the sizes of particles and species of dyes, which is quite important for the applications of PLPCs.

2.5. Photonic Patterns for Anti-Counterfeiting. The dual-mode optical colors of PLPCs inspire us to develop a new way to encrypt PC patterns for anti-counterfeiting. For example, the PC patterns can be fabricated by the combination of the self-assembly of dye-doped and SiO_2 particles (Figure 4a). Here, the photonic pattern was obtained by the assembly of PLPCs from R−SiO_2 particles and PCs from SiO_2 particles into the permutation and combination composed of 3 × 5 circular grids, in which the reflection peaks, structural colors, and angle dependence of the grids can be independently controlled in the desired way. As presented in Figure 4b (left), under normal conditions, each grid shows similar blue color, and there is no obvious difference in their structural colors because of similar sizes of R−SiO_2 and SiO_2 particles. When the pattern is illuminated by UV light, the grids with PLPCs show strong red PL colors, while grids with PCs do not exhibit PL color, resulting in a red "E" pattern (Figure 4b, right). After turning off, the red "E" disappears, and the PC pattern recovers to the pristine state. The color switch between the pristine and UV illuminated state is fully reversible.

https://doi.org/10.1021/acsomega.1c07150
ACS Omega 2022, 7, 7320−7326

Except for the single PL color encryption, the PC pattern with multi-PL colors can also be easily fabricated through a similar approach. As shown in Figure 4c, the big flower, small flower, and the leaves of the pattern are assembled from the R−SiO_2, R−SiO_2, F−SiO_2, and F−SiO_2 particles, respectively. Under ambient light, each region of the pattern shows similar structural colors, apparently due to similar sizes of the particles. In contrast, the patterns exhibit green, yellow, and red PL colors under UV illumination. The combination of structural and PL colors will extend the applications of PCs in the field of anti-counterfeiting, information protection, and displays.

3. CONCLUSIONS

In summary, PLPCs with brilliant structural and PL colors were fabricated by the self-assembly of organic dye-doped silica particles into ordered structures. The structural color of the PLPC can be adjusted by altering the size of dye-doped silica particles. The PL color of PLPCs can be well-controlled by altering the species of dyes or by mixing of silica particles with different dyes. Based on these advantages, encrypted photonic patterns were fabricated by the combinations of PLPCs with similar reflection wavelengths and structural colors but different PL colors. The information of photonic patterns can be hidden at normal conditions but instantly and reversibly revealed under UV illumination. The simple and efficient fabrications, together with the tunable structural and PL colors of PLPCs will facilitate the applications of PCs in the field of displays, information protection, and anti-counterfeiting.

4. EXPERIMENTAL SECTION

4.1. Materials. FITC and RITC were purchased from Sigma-Aldrich. TEOS (98%), ethanol (EtOH, 99%), and aqueous ammonia (28%) were purchased from J&K. Poly(ethylene glycol) methacrylate (Mn: 360), poly(ethylene glycol) diacrylate (Mn: 250), and 2-hydroxy-2-methylpropiophenone (photo-initiator, 97%) were obtained from Sigma-Aldrich. All the chemicals are used as received without further purifications.

4.2. Synthesis of SiO_2, F−SiO_2, and R−SiO_2 Particles. FTIC (0.1 mmol) or RITC (0.02 mmol) was dissolved into the mixture of ethanol (20 mL) and APS (0.2 mL), respectively. The mixed solutions were stirred for 12 h to form APS−FITC or APS−RITC precursors before usage. Afterward, TEOS (64 mL) and the APS−FITC (20 mL) [or APS−RITC solution (20 mL)] precursor solution were added into the mixture containing ethanol (800 mL), H_2O (56 mL), and NH_4OH (32 mL). After stirring for 5 h, the products were purified by the centrifugation−washing process with excessive ethanol. The FITC- and RITC-doped silica particles are named as F−SiO2 and R−SiO2 particles, respectively. The stöber silica particles were synthesized by similar procedures with TEOS as the saline resource.

4.3. Fabrication of PLPCs. The F−SiO_2 or R−SiO_2 particles are dispersed into ethanol in a concentration of 100 mg/mL. Then, 0.05 mL of solution was cast onto the glass, which was dried at 333 K for 10 min. PLPCs with brilliant colors can be achieved after evaporation of ethanol.

4.4. Characterization. The morphology of F−SiO_2, R−SiO_2, and SiO_2 and the assembly structures of PCs were investigated by the HITACHI SEM-SU8010. The optical microscopy images and microscopic reflectance spectra were obtained on an Olympus BXFM reflection-type microscope operated in the dark field mode. The reflectance and backscattering spectra at different angles were measured using a NOVA spectrometer (Hamamatsu, S7031). The UV−vis absorption spectra were recorded on a SHIMADZU UV-3600Plus spectrophotometer. The PL spectrum was recorded on a HORIBA Instruments Incorporated Fluorolog-3 instrument.

■ ASSOCIATED CONTENT

Supporting Information

The Supporting Information is available free of charge at https://pubs.acs.org/doi/10.1021/acsomega.1c07150.

SEM images and corresponding PL spectra of R−SiO_2 particles with different sizes (PDF)

■ AUTHOR INFORMATION

Corresponding Authors

Dongpeng Yang − *School of Materials and Energy, School of Physics and Optoelectric Engineering, Guangzhou Key Laboratory of Low-Dimensional Materials and Energy Storage Devices, Guangdong University of Technology, Guangzhou 510006, P. R. China;* orcid.org/0000-0002-6950-5985; Email: dpyang@gdut.edu.cn

Li Luo − *School of Materials and Energy, School of Physics and Optoelectric Engineering, Guangzhou Key Laboratory of Low-Dimensional Materials and Energy Storage Devices, Guangdong University of Technology, Guangzhou 510006, P. R. China*; Email: luoli@gdut.edu.cn

Shaoming Huang − *School of Materials and Energy, School of Physics and Optoelectric Engineering, Guangzhou Key Laboratory of Low-Dimensional Materials and Energy Storage Devices, Guangdong University of Technology, Guangzhou 510006, P. R. China;* orcid.org/0000-0003-0242-1143; Email: smhuang@gdut.edu.cn

Authors

Chenjing Xu − *School of Materials and Energy, School of Physics and Optoelectric Engineering, Guangzhou Key Laboratory of Low-Dimensional Materials and Energy Storage Devices, Guangdong University of Technology, Guangzhou 510006, P. R. China*

Changgeng Huang − *School of Materials and Energy, School of Physics and Optoelectric Engineering, Guangzhou Key Laboratory of Low-Dimensional Materials and Energy Storage Devices, Guangdong University of Technology, Guangzhou 510006, P. R. China*

Complete contact information is available at: https://pubs.acs.org/10.1021/acsomega.1c07150

Notes

The authors declare no competing financial interest.

■ ACKNOWLEDGMENTS

This work was financially supported by the National Natural Science Foundation of China (21673160, 51920105004, 51372173, and 11574058), the Guangzhou Key Laboratory of Low Dimensional Materials and Energy Storage Devices (20195010002), and the General Program of the Natural Science Foundation of Guangdong Province (2019A1515011563).

REFERENCES

(1) von Freymann, G.; Kitaev, V.; Lotsch, B. V.; Ozin, G. A. Bottom-up assembly of photonic crystals. *Chem. Soc. Rev.* **2013**, *42*, 2528−2554.

(2) Hou, J.; Li, M.; Song, Y. Patterned Colloidal Photonic Crystals. *Angew. Chem., Int. Ed.* **2018**, *57*, 2544−2553.

(3) Wu, S.; Xia, H.; Xu, J.; Sun, X.; Liu, X. Manipulating Luminescence of Light Emitters by Photonic Crystals. *Adv. Mater.* **2018**, *30*, 1803362.

(4) Arsenault, A. C.; Puzzo, D. P.; Manners, I.; Ozin, G. A. Photonic-crystal full-colour displays. *Nat. Photonics* **2007**, *1*, 468−472.

(5) Puzzo, D. P.; Arsenault, A. C.; Manners, I.; Ozin, G. A. Electroactive Inverse Opal: A Single Material for All Colors. *Angew. Chem., Int. Ed.* **2009**, *48*, 943−947.

(6) Lee, I.; Kim, D.; Kal, J.; Baek, H.; Kwak, D.; Go, D.; Kim, E.; Kang, C.; Chung, J.; Jang, Y.; Ji, S.; Joo, J.; Kang, Y. Quasi-Amorphous Colloidal Structures for Electrically Tunable Full-Color Photonic Pixels with Angle-Independency. *Adv. Mater.* **2010**, *22*, 4973−4977.

(7) Lee, S. Y.; Kim, S.-H.; Hwang, H.; Sim, J. Y.; Yang, S.-M. Controlled Pixelation of Inverse Opaline Structures Towards Reflection- Mode Displays. *Adv. Mater.* **2014**, *26*, 2391−2397.

(8) Yang, D.; Ye, S.; Ge, J. From Metastable Colloidal Crystalline Arrays to Fast Responsive Mechanochromic Photonic Gels: An Organic Gel for Deformation-Based Display Panels. *Adv. Funct. Mater.* **2014**, *24*, 3197−3205.

(9) Fu, Q.; Zhu, H.; Ge, J. Electrically Tunable Liquid Photonic Crystals with Large Dielectric Contrast and Highly Saturated Structural Colors. *Adv. Funct. Mater.* **2018**, *28*, 1804628.

(10) Yan, Z.; Zhang, Z.; Wu, W.; Ji, X.; Sun, S.; Jiang, Y.; Tan, C. C.; Yang, L.; Chong, C. T.; Qiu, C.-W.; Zhao, R. Floating solid-state thin films with dynamic structural colour. *Nat. Nanotechnol.* **2021**, *16*, 795−801.

(11) Kim, H.; Ge, J.; Kim, J.; Choi, S.-e.; Lee, H.; Lee, H.; Park, W.; Yin, Y.; Kwon, S. Structural colour printing using a magnetically tunable and lithographically fixable photonic crystal. *Nat. Photonics* **2009**, *3*, 534−540.

(12) Fang, Y.; Ni, Y.; Leo, S.-Y.; Taylor, C.; Basile, V.; Jiang, P. Reconfigurable photonic crystals enabled by pressure-responsive shape-memory polymers. *Nat. Commun.* **2015**, *6*, 7416.

(13) Lee, J.-S.; Je, K.; Kim, S.-H. Designing Multicolored Photonic Micropatterns through the Regioselective Thermal Compression of Inverse Opals. *Adv. Funct. Mater.* **2016**, *26*, 4587−4594.

(14) Chen, K.; Fu, Q.; Ye, S.; Ge, J. Multicolor Printing Using Electric-Field-Responsive and Photocurable Photonic Crystals. *Adv. Funct. Mater.* **2017**, *27*, 1702825.

(15) Gao, M.; Li, L.; Song, Y. Inkjet printing wearable electronic devices. *J. Mater. Chem. C* **2017**, *5*, 2971−2993.

(16) Wu, Y.; Ren, J.; Zhang, S.; Wu, S. Nanosphere-Aggregation-Induced Reflection and Its Application in Large-Area and High-Precision Panchromatic Inkjet Printing. *ACS Appl. Mater. Interfaces* **2020**, *12*, 10867−10874.

(17) Yang, D.; Ye, S.; Ge, J. Old relief printing applied to the current preparation of multi-color and high resolution colloidal photonic crystal patterns. *Chem. Commun.* **2015**, *51*, 16972−16975.

(18) Takeoka, Y.; Yoshioka, S.; Takano, A.; Arai, S.; Nueangnoraj, K.; Nishihara, H.; Teshima, M.; Ohtsuka, Y.; Seki, T. Production of Colored Pigments with Amorphous Arrays of Black and White Colloidal Particles. *Angew. Chem., Int. Ed.* **2013**, *52*, 7261−7265.

(19) Lee, H. S.; Kim, J. H.; Lee, J.-S.; Sim, J. Y.; Seo, J. Y.; Oh, Y.-K.; Yang, S.-M.; Kim, S.-H. Magnetoresponsive Discoidal Photonic Crystals Toward Active Color Pigments. *Adv. Mater.* **2014**, *26*, 5801−5807.

(20) Li, Q.; Zhang, Y.; Shi, L.; Qiu, H.; Zhang, S.; Qi, N.; Hu, J.; Yuan, W.; Zhang, X.; Zhang, K.-Q. Additive Mixing and Conformal Coating of Noniridescent Structural Colors with Robust Mechanical Properties Fabricated by Atomization Deposition. *ACS Nano* **2018**, *12*, 3095−3102.

(21) Hu, Y.; Yang, D.; Huang, S. Amorphous Photonic Structures with Brilliant and Noniridescent Colors via Polymer-Assisted Colloidal Assembly. *ACS Omega* **2019**, *4*, 18771−18779.

(22) Yang, D.; Luo, W.; Huang, Y.; Huang, S. Facile Synthesis of Monodispersed SiO_2@Fe_3O_4 Core-Shell Colloids for Printing and Three-Dimensional Coating with Noniridescent Structural Colors. *ACS Omega* **2019**, *4*, 528−534.

(23) Yang, X.; Yang, D.; Chen, Y.; Hu, Y.; Huang, S. Highly Efficient Fabricating Amorphous Photonic Crystals Using Less Polar Solvents and the Wettability-Based Information Storage and Recognition. *Part. Part. Syst. Charact.* **2020**, *37*, 2000043.

(24) Li, B.; Ouyang, C.; Yang, D.; Ye, Y.; Ma, D.; Luo, L.; Huang, S. Noniridescent structural color from enhanced electromagnetic resonances of particle aggregations and its applications for reconfigurable patterns. *J. Colloid Interface Sci.* **2021**, *604*, 178−187.

(25) Hu, Y.; Zhang, Y.; Yang, D.; Ma, D.; Huang, S. Self-assembly of colloidal particles into amorphous photonic crystals. *Mater. Adv.* **2021**, *2*, 6499−6518.

(26) Yue, Y. F.; Haque, M. A.; Kurokawa, T.; Nakajima, T.; Gong, J. P. Lamellar Hydrogels with High Toughness and Ternary Tunable Photonic Stop-Band. *Adv. Mater.* **2013**, *25*, 3106−3110.

(27) Bai, L.; Xie, Z.; Wang, W.; Yuan, C.; Zhao, Y.; Mu, Z.; Zhong, Q.; Gu, Z. Bio-Inspired Vapor-Responsive Colloidal Photonic Crystal Patterns by Inkjet Printing. *ACS Nano* **2014**, *8*, 11094−11100.

(28) Zhang, Y.; Fu, Q.; Ge, J. Photonic sensing of organic solvents through geometric study of dynamic reflection spectrum. *Nat. Commun.* **2015**, *6*, 7510.

(29) Zhu, B.; Fu, Q.; Chen, K.; Ge, J. Liquid Photonic Crystals for Mesopore Detection. *Angew. Chem., Int. Ed.* **2018**, *57*, 252−256.

(30) Hu, Y.; Zhang, Y.; Chen, T.; Yang, D.; Ma, D.; Huang, S. Highly Efficient Detection of Homologues and Isomers by the Dynamic Swelling Reflection Spectrum. *ACS Appl. Mater. Interfaces* **2020**, *12*, 45174−45183.

(31) Kou, D.; Ma, W.; Zhang, S. Functionalized Mesoporous Photonic Crystal Film for Ultrasensitive Visual Detection and Effective Removal of Mercury (II) Ions in Water. *Adv. Funct. Mater.* **2021**, *31*, 2007032.

(32) Hu, Y.; Yang, D.; Ma, D.; Huang, S. Extremely sensitive mechanochromic photonic crystals with broad tuning range of photonic bandgap and fast responsive speed for high-resolution multicolor display applications. *Chem. Eng. J.* **2022**, *429*, 132342.

(33) Yang, D.; Qin, Y.; Ye, S.; Ge, J. Polymerization-Induced Colloidal Assembly and Photonic Crystal Multilayer for Coding and Decoding. *Adv. Funct. Mater.* **2014**, *24*, 817−825.

(34) Li, Y.; Zhou, X.; Yang, Q.; Li, Y.; Li, W.; Li, H.; Chen, S.; Li, M.; Song, Y. Patterned photonic crystals for hiding information. *J. Mater. Chem. C* **2017**, *5*, 4621−4628.

(35) Qi, Y.; Niu, W.; Zhang, S.; Wu, S.; Chu, L.; Ma, W.; Tang, B. Encoding and Decoding of Invisible Complex Information in a Dual-Response Bilayer Photonic Crystal with Tunable Wettability. *Adv. Funct. Mater.* **2019**, *29*, 1906799.

(36) Ouyang, C.; Zhang, Y.; Yang, D.; Ma, D.; Huang, S. A new coding-decoding system through combining near-infrared photonic crystals and their spatial reflection spectra. *J. Mater. Chem. C* **2021**, *9*, 4466−4473.

(37) Zhou, M.; Wu, H. B.; Bao, J.; Liang, L.; Lou, X. W. D.; Xie, Y. Ordered Macroporous BiVO4 Architectures with Controllable Dual Porosity for Efficient Solar Water Splitting. *Angew. Chem., Int. Ed.* **2013**, *52*, 8579−8583.

(38) Yu, W.-Y.; Ma, D.-K.; Yang, D.-P.; Yang, X.-G.; Xu, Q.-L.; Chen, W.; Huang, S. Highly efficient utilization of light and charge separation over a hematite photoanode achieved through a non-contact photonic crystal film for photoelectrochemical water splitting. *Phys. Chem. Chem. Phys.* **2020**, *22*, 20202−20211.

(39) Lee, H. S.; Shim, T. S.; Hwang, H.; Yang, S.-M.; Kim, S.-H. Colloidal Photonic Crystals toward Structural Color Palettes for Security Materials. *Chem. Mater.* **2013**, *25*, 2684−2690.

(40) Chen, K.; Zhang, Y.; Ge, J. Highly Invisible Photonic Crystal Patterns Encrypted in an Inverse Opaline Macroporous Polyurethane

https://doi.org/10.1021/acsomega.1c07150
ACS Omega 2022, 7, 7320−7326

Film for Anti-Counterfeiting Applications. *ACS Appl. Mater. Interfaces* **2019**, *11*, 45256−45264.
(41) Wu, S.; Liu, T.; Tang, B.; Li, L.; Zhang, S. Different Structural Colors or Patterns on the Front and Back Sides of a Multilayer Photonic Structure. *ACS Appl. Mater. Interfaces* **2019**, *11*, 27210−27215.
(42) Wu, S.; Liu, T.; Tang, B.; Li, L.; Zhang, S. Structural Color Circulation in a Bilayer Photonic Crystal by Increasing the Incident Angle. *ACS Appl. Mater. Interfaces* **2019**, *11*, 10171−10177.
(43) Liu, F.; Zhang, S.; Meng, Y.; Tang, B. Thermal Responsive Photonic Crystal Achieved through the Control of Light Path Guided by Phase Transition. *Small* **2020**, *16*, 2002319.
(44) Qi, Y.; Niu, W.; Zhang, S.; Zhang, Z.; Wu, S.; Ma, W. Rotational Periodicity Display of the Tunable Wettability Pattern in a Photoswitch Based on a Response Bilayer Photonic Crystal. *ACS Appl. Mater. Interfaces* **2020**, *12*, 9664−9672.
(45) Hu, Y.; Yang, D.; Huang, S. Simple and Ultrafast Fabrication of Invisible Photonic Prints with Reconfigurable Patterns. *Adv. Optical Mater.* **2020**, *8*, 1901541.
(46) Yang, D.; Ouyang, C.; Zhang, Y.; Ma, D.; Huang, S. Rapid Fabrication of Alcohol Responsive Photonic Prints with Changeable Color Contrasts for Anti-Counterfeiting Application. *Adv. Mater. Interfaces* **2021**, *8*, 2001905.
(47) Yang, D.; Ouyang, C.; Zhang, Y.; Ma, D.; Ye, Y.; Bu, D.; Huang, S. Simple and efficient fabrication of multi-stage color-changeable photonic prints as anti-counterfeit labels. *J. Colloid Interface Sci.* **2021**, *590*, 134−143.
(48) Yang, D.; Liao, G.; Huang, S. Hand Painting of Noniridescent Structural Multicolor through the Self-Assembly of $YOHCO_3$ Colloids and Its Application for Anti-Counterfeiting. *Langmuir* **2019**, *35*, 8428−8435.
(49) Yang, D.; Liao, G.; Huang, S. Invisible photonic prints shown by UV illumination: combining photoluminescent and noniridescent structural colors. *J. Mater. Chem. C* **2019**, *7*, 11776−11782.

https://doi.org/10.1021/acsomega.1c07150
ACS Omega 2022, 7, 7320−7326